

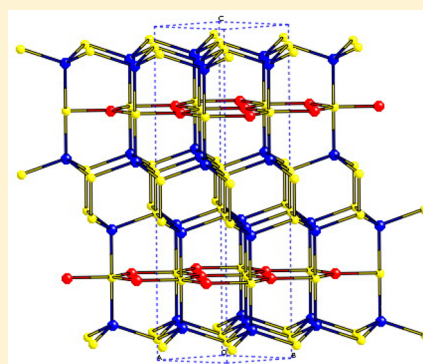
# Nature of Holes, Oxidation States, and Hypervalency in Covellite (CuS)

Sergio Conejeros,<sup>†</sup> Ibério de P. R. Moreira,<sup>†</sup> Pere Alemany,<sup>\*,†</sup> and Enric Canadell<sup>\*,‡</sup>

<sup>†</sup>Departament de Química Física and Institut de Química Teòrica i Computacional (IQTCUB), Universitat de Barcelona, Martí i Franquès 1, 08028 Barcelona, Spain

<sup>‡</sup>Institut de Ciència de Materials de Barcelona (CSIC), Campus de la UAB, 08193 Bellaterra, Spain

**ABSTRACT:** The electronic structure of covellite (CuS) is analyzed on the basis of density functional theory calculations. The nature of holes in the valence band, as well as the so far much debated question of the appropriate oxidation formalism for this conductor, is discussed. The role of S–S bonds and the anomalous coordination of one type of sulfur atom (hypervalency) are considered. It is suggested that the low-temperature transition is mostly a symmetry-lowering process slightly stabilizing the Cu–S network.



## INTRODUCTION

Covellite is a blue-indigo binary copper sulfide (CuS) that has recently attracted considerable attention because of its potential interest in optics, electronic and photovoltaic devices, rechargeable lithium batteries, and catalysis.<sup>1</sup> It exhibits a metallic behavior, becoming a superconductor at 1.6 K.<sup>2,3</sup> Its remarkable room temperature hexagonal crystal structure (Figure 1, left)<sup>2</sup> can be described as a succession of planar CuS layers and Cu<sub>2</sub>S<sub>2</sub> double layers. In the former, the Cu(1) atoms occur in a trigonal-planar coordination environment, whereas those of the double layers, Cu(2), are tetrahedrally coordinated with three S(2) atoms of the double layer and one sulfur atom of the adjacent planar layer, S(1). At 55 K, the system undergoes a structural transition from a hexagonal to an orthorhombic structure<sup>2</sup> (Figure 1, right), which does not seem to noticeably alter the electrical and magnetic properties.<sup>4</sup> A comparison of the two crystal structures of CuS determined at 8 and 295 K shows that the structural phase transition involves a slight slipping of the CuS layers with respect to the Cu<sub>2</sub>S<sub>2</sub> double layers, implying only a small distortion of the local coordination environments.

The high-temperature structure<sup>2</sup> of CuS exhibits several intriguing features. First, the S(2) atoms in the double layers occur in S–S pairs with a 1.997 Å distance, clearly suggesting the occurrence of a single bond. Second, the S(1) atom is pentacoordinated with bond lengths of 3 × 2.190 and 2 × 2.334 Å. Although the apical distances are somewhat longer than the basal ones, they are comparable to the remaining bond lengths in the Cu(2)S<sub>4</sub> tetrahedra, 3 × 2.315 Å. These observations bring to the fore the important question of what is the appropriate oxidation formalism for this system, an essential step in developing an intuitive understanding of the physical

properties of covellite and how they are related to the details of the crystal structure. The principal structural features [local coordinations of Cu(1) and Cu(2) atoms and the presence of S–S bonds] remain practically unaffected by the structural transition at 55 K so that the structural transition is not expected to induce a major change in the oxidation formalism. We thus have found it convenient to focus first our attention on the electronic structure of the hexagonal phase and discuss afterward the effects of the symmetry lowering on it to try to shed some light on the driving force behind the observed transition.

The complex crystal structure with two totally different crystallographic sites for copper and sulfur, respectively, gives us already a hint that, despite its apparently simple stoichiometry, establishing a satisfactory oxidation formalism for covellite is not an easy task. This is confirmed by the trouble caused by the ease of oxidation of sulfide S<sup>2-</sup> in the assignment of oxidation states for copper and sulfur in molecular compounds.<sup>5</sup>

Several possible oxidation formalisms have been suggested in the past for CuS. On the basis of structural observations, Fjellvag et al.<sup>2</sup> suggested (Cu<sup>+</sup>)<sub>3</sub>(S<sub>2</sub><sup>2-</sup>)(S<sup>-</sup>). Later Liang and Whangbo<sup>6</sup> criticized this description, proposing (Cu<sup>+</sup>)<sub>3</sub>(S<sub>2</sub><sup>-</sup>)(S<sup>2-</sup>) as more appropriate. Recently, Mazin<sup>7</sup> proposed (Cu<sup>4/3+</sup>)<sub>3</sub>(S<sub>2</sub><sup>2-</sup>)(S<sup>2-</sup>) on the basis of density functional theory (DFT) calculations, and Kumar et al.<sup>8</sup> suggested [(Cu<sub>Td</sub>)<sub>2</sub>]<sup>3+</sup>(Cu<sub>T</sub>)<sup>+</sup>(S<sub>2</sub><sup>2-</sup>)(S<sup>2-</sup>) on the basis of spectroscopic data. Thus, there is considerable confusion in the literature, and, more importantly, none of these descriptions has been

Received: July 21, 2014

Published: November 14, 2014

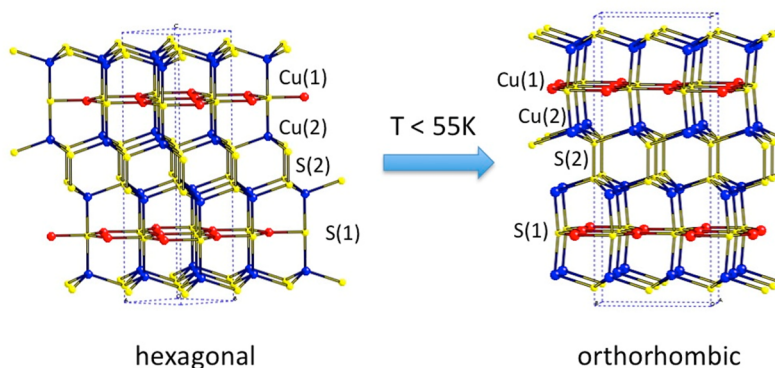


**Figure 1.** Hexagonal (room temperature) and orthorhombic (low temperature) crystal structures of covellite.

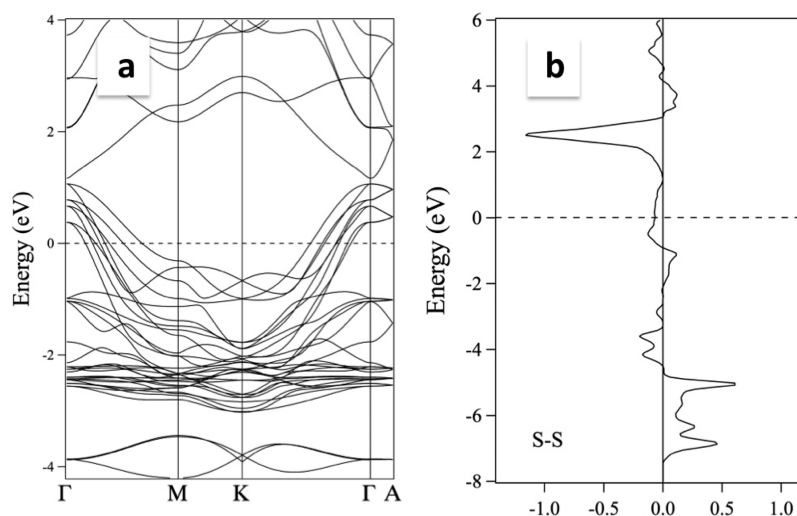


**Figure 2.** (a) Calculated band structure for hexagonal covellite, where  $\Gamma = (0, 0, 0)$ ,  $M = (\frac{1}{2}, 0, 0)$ ,  $K = (\frac{1}{3}, \frac{1}{3}, 0)$ , and  $A = (0, 0, \frac{1}{2})$  in units of the reciprocal lattice vectors. (b) COOP curve for the S(2)–S(2) pair.

clearly correlated with the details of the crystal structure. A correct description of this material should be consistent with both the details of the crystal structure [the presence of pentacoordinated S(1) and S–S bonds] and those of the band structure (origin of the metallic state, number and shape of the partially filled bands, etc.). In what follows, we report what we believe is the simplest description of the relationship between the crystal and electronic features for this intriguing material based on first-principles band-structure calculations.

## ■ COMPUTATIONAL DETAILS

First-principles spin-polarized calculations were carried out using a numerical atomic orbitals DFT approach<sup>9</sup> developed for efficient calculations in large systems and implemented in the *SIESTA* code.<sup>10–12</sup> We have used the generalized gradient approximation to DFT and, in particular, the functional of Perdew, Burke, and Ernzerhof (PBE).<sup>13</sup> Only the valence electrons are considered in the calculation, with the core being replaced by norm-conserving scalar-relativistic pseudopotentials<sup>14</sup> factorized in the Kleinman–Bylander form.<sup>15</sup> We have used a split-valence double- $\zeta$  basis set including polarization orbitals, as obtained with an energy shift of 100 meV for all atoms.<sup>16</sup> The energy cutoff of the real-space integration mesh was 150 Ry, and the Brillouin zone was sampled using grids<sup>17</sup> of  $12 \times 12 \times 12$   $k$  points for calculation of the band structures and  $20 \times 20 \times 20$   $k$  points for calculation of the Fermi surface. All calculations presented were performed using the experimental geometries.

Because a small residual magnetic moment of 0.24–0.30  $\mu_B$  has been reported for some natural samples of covellite,<sup>2</sup> we have used

spin-polarized calculations to obtain reasonable solutions with unpaired electrons on copper, but all of them turned out to be higher in energy than the metallic solution, which we assume to properly describe the ground state in CuS. The reported residual magnetic moment could be due to the presence of paramagnetic impurities in the analyzed samples, Pauli paramagnetism or excited state magnetism.

As suggested in the literature,<sup>18</sup> we also performed calculations by applying a Hubbard correction term<sup>19</sup>  $U = 5$  eV for the 3d electrons of copper to the PBE calculation (DFT +  $U$ ).<sup>20</sup> Calculations including this correction give a band-structure diagram in the region around the Fermi level that is practically indistinguishable from that obtained without them. This is an indication that considering corrections for the repulsion on the 3d electrons of copper does not have significant consequences on the bonding and oxidation formalism of CuS, which is the central focus of this article, and for this reason, we will not further discuss the results of these calculations in the following.

## ■ RESULTS AND DISCUSSION

The calculated band structure near the Fermi level for the hexagonal phase of CuS is shown in Figure 2a. There are four pairs of partially filled bands occurring around the  $\Gamma$  point. These are dispersive along the  $\Gamma$ – $M$  and  $\Gamma$ – $K$  directions, but they exhibit an almost negligible dispersion along the  $\Gamma$ – $A$  direction (i.e., the  $c^*$  direction). Thus, there are four pairs of two-dimensional (2D) partially filled bands, and conduction should be strongly anisotropic, with better conductivity along the hexagonal planes.

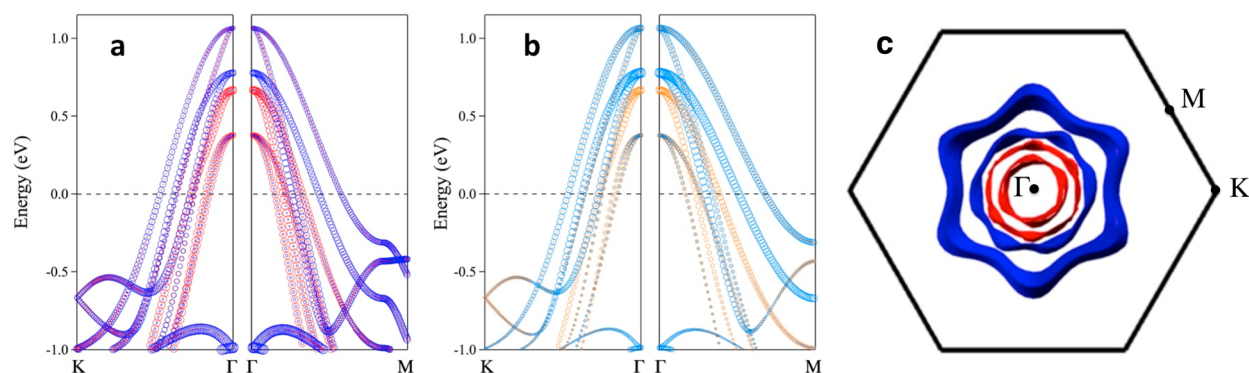


**Figure 3.** Band structure along selected lines for hexagonal covellite, where the size of the circles is proportional to the participation of the different orbitals in the band. (a) Red and blue circles referring to the 3d orbitals of Cu(1) and Cu(2), respectively. (b) Yellow and light-blue circles referring to the 3p orbitals of S(1) and S(2), respectively. (c) Calculated Fermi surface viewed along the  $c$  axis, where  $\Gamma = (0, 0, 0)$ ,  $M = (\frac{1}{2}, 0, 0)$ , and  $K = (\frac{1}{3}, \frac{1}{3}, 0)$  in units of the reciprocal lattice vectors. Branches in blue are mainly associated with the  $(\text{Cu}_{\text{Td}}\text{S})_2$  double layers and those in red with the  $\text{Cu}_{\text{T}}\text{S}$  single layers.

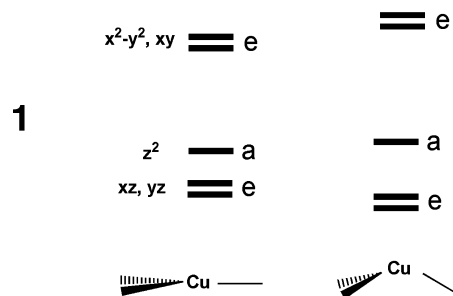
Let us note that, although the chemical repeat unit,  $\text{Cu}_3\text{S}_3$ , is made of three layers, the unit cell of the solid,  $\text{Cu}_6\text{S}_6$ , contains twice the chemical unit. The composition of these partially filled bands is analyzed in Figure 3, where the participation of the 3d orbitals of the two different copper atoms and that of the 3p orbitals of the two different sulfur atoms are highlighted. Several conclusions can be reached from this figure. First, the copper and sulfur orbitals strongly mix in the partially filled bands. Second, the two upper pairs of partially filled bands are mostly associated with the layers containing the tetrahedrally coordinated Cu(2) atoms. Third, the two lower pairs of partially filled bands are mostly associated with the layers containing the trigonal-planar-coordinated Cu(1) atoms. This leads to a Fermi surface (Figure 3c) that is in good agreement with those published previously<sup>6,7</sup> in which each pair of bands crossing the Fermi level gives a more or less warped cylindrical surface centered around  $\Gamma$  and extending along the  $c^*$  direction.

The next question to ask before considering the actual oxidation formalism is the role of the S(2)–S(2) pairs. Shown in Figure 2b is a crystal orbital overlap population (COOP) curve for this atom pair, exhibiting a large positive (i.e., bonding) contribution between  $-7$  and  $-5$  eV associated with the bonding states, a wide region with small contributions, and finally, well above the Fermi level, around 2.5 eV, a large negative contribution associated with the unoccupied antibonding states of the pair. This, together with the large calculated overlap population  $0.4e^-$  between the two neighboring S(2) atoms, points clearly to the presence of an S–S single bond in the structure of covellite. Consequently, each pair of S(2) atoms in covellite should be considered as  $\text{S}_2^{2-}$  for the purpose of assigning oxidation states.

The key structural feature in discussing (i) the appropriate oxidation formalism, (ii) the occurrence of five bonds around S(1), (iii) why there are two partially filled bands per chemical unit, whereas there are three copper and three sulfur atoms, and (iv) why the structure distorts at low temperature is that all atoms in the hexagonal structure occur along 3-fold symmetry axes. Consequently, all relevant orbitals must be of either the a-type (nondegenerate) or e-type (doubly degenerate).

Let us consider covellite as resulting from the interaction of the planar and double layers. The d-orbital splittings for a transition-metal atom in trigonal-planar and trigonal-pyramidal coordination are shown in **1**, where  $z$  is coincident with the direction of the 3-fold axes.<sup>21</sup> In both cases, the upper Cu–S

antibonding levels are of e-type symmetry. Thus, the upper levels of the planar layers result from the interaction between an e-type pair of S(1) ( $3p_x, 3p_y$ ) and an e-type pair of Cu(1). One of the two remaining a-type orbitals ( $3s$ ) is used to establish the third  $\sigma$  bond, and finally the  $3p_z$  orbital is of the a-type but antisymmetric with respect to the planar layer. Because there are no Cu 3d orbitals of the same symmetry, it cannot contribute to the bonding within the layer. For the time being, we may conclude that *each planar layer will give rise to one pair of high-lying bands built from these locally e-type orbitals.*



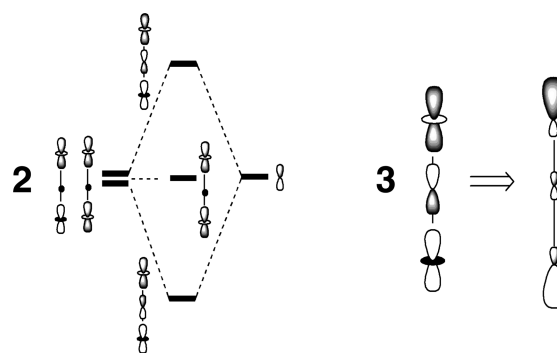
Let us now turn to the double layers. One of the a-type orbitals of S(2) is used to form the S–S bond, and the three remaining ones, a + e, are used in the bonding and antibonding interactions with the Cu(2) 3d orbitals. As shown in **1**, the upper antibonding levels are a pair of e-type orbitals. Because there are two individual layers, there are also two pairs of these e-type orbitals from which we can build in-phase and out-of-phase combinations. The orbitals of the two layers interact through  $\pi$ -type interactions along the S–S bonds so that one of the two sets is stabilized and the other is further destabilized. Consequently, *each double layer has one pair of high-lying bands built from the locally e-type orbitals.* Because the repeat unit of hexagonal covellite contains two double and two single layers, we are led to the conclusion that if the different types of layers would not interact, the upper bands of the system should be four pairs of these e-based bands.

We must, however, consider the interaction between layers. This interaction is switched on when the a-type S(1)  $3p_z$  orbitals, which are not used for intralayer bonding, are allowed to interact with the  $z^2$ -like a-type orbital of the Cu(2) atoms (see **1**), which are ideally oriented toward each other. Each S(1)  $3p_z$  orbital can interact with two of these orbitals. We can

thus create in-phase and out-of-phase combinations of these  $z^2$ -like orbitals, but only the out-of-phase ones can interact with the S(1)  $3p_z$  orbital, leading to bonding and antibonding combinations (2). Thus, there is one high-lying antibonding  $a$ -type orbital per planar layer.

Covellite has  $17 \times 6 = 102$  valence electrons per  $(\text{CuS})_6$  repeat unit. The number of valence bands below the small gap around 1 eV in Figure 2 is given by the total number of the 3s and 3p orbitals of the sulfur atoms plus the total number of 3d orbitals of the copper atoms minus the number of S(2)–S(2)  $\sigma^*$  orbitals, i.e.,  $(6 \times 4) + (6 \times 5) - 2 = 52$ . Consequently, there are two holes to be placed in the upper part of the valence bands of covellite. Our analysis shows that four pairs of  $e$ -type bands (one per planar layer and one per double layer) and two  $a$ -type bands (one per planar layer) must be in the region around the Fermi level. The question now is, how are the holes distributed among these bands? The  $e$ -type bands are doubly degenerate at  $\Gamma$ , whereas the  $a$ -type ones are not. Figure 3 clearly shows that the partially filled bands of covellite correspond to the four predicted pairs of  $e$ -type bands (degenerate at the  $\Gamma$  point). Because from our analysis it follows that all antibonding Cu–S  $e$ -type bands are 2D bands delocalized along the planes perpendicular to the  $c$  direction, we must conclude that the two holes are completely delocalized among the Cu–S planes of the structure. In addition, the Fermi surface of covellite must be composed of four pairs of cylinders parallel to the  $c$  direction (Figure 3c). Because the two pairs of bands of the double layers are higher in energy than those of the single layers and thus contain a larger proportion of holes (around twice), we can conclude that the two holes are almost equally distributed among the six layers of the repeat unit. We thus conclude that each layer in covellite contains approximately  $1/3$  electron per repeat unit, completely delocalized among the copper and sulfur atoms so that a description in terms of integer oxidation states is not pertinent in this case.

At this point, it must be recognized that the above discussion apparently leads to a serious conceptual problem. If only the  $e$ -type bands contain holes, all  $a$ -type bands based on the three orbitals shown in 2 should be completely filled and we are led



to the conclusion that there should be no bonds between the double and single CuS layers. This is obviously not the case, as is clearly illustrated by the Cu(2)–S(1) distance, which is comparable to the Cu(2)–S(2) one and the values of the corresponding overlap populations, 0.203 and 0.271, that have also similar magnitudes. The puzzle is easily unraveled by recalling that in copper the 4s and 4p orbitals are rather low in energy and mix noticeably into the valence levels, leading sometimes to unexpected bonding situations such as the so-called  $d^{10}\dots d^{10}$  interactions,<sup>22</sup> which have been shown to have noticeable consequences in the electronic structure of a material.<sup>23</sup> The linear geometry in CuS is very favorable for participation of the Cu  $4p_z$  orbitals in the orbital interaction in 2. The in-phase combination of these orbitals mixes substantially into the upper level that becomes essentially nonbonding (3), explaining why it does not hold any hole. Consequently, the two upper levels of the Cu(2)–S(1)–Cu(2) three-center interaction are essentially nonbonding (they lead to four levels in the bunch of bands between  $-1$  and  $-2$  eV in the band structure of Figure 2a), while the lower level is Cu–S bonding. Cohesion between layers is thus handled by two-electron three-center bonding as in any hypervalent system.<sup>21</sup> Note that the hypervalency implies an  $\text{S}^{2-}$  formal oxidation state for S(1). We thus can conclude that the generation of S–S bonds and the hypervalency leave the system with just two holes per repeat unit (one per chemical unit), which are shared almost equally by the different hexagonal layers of the structure.

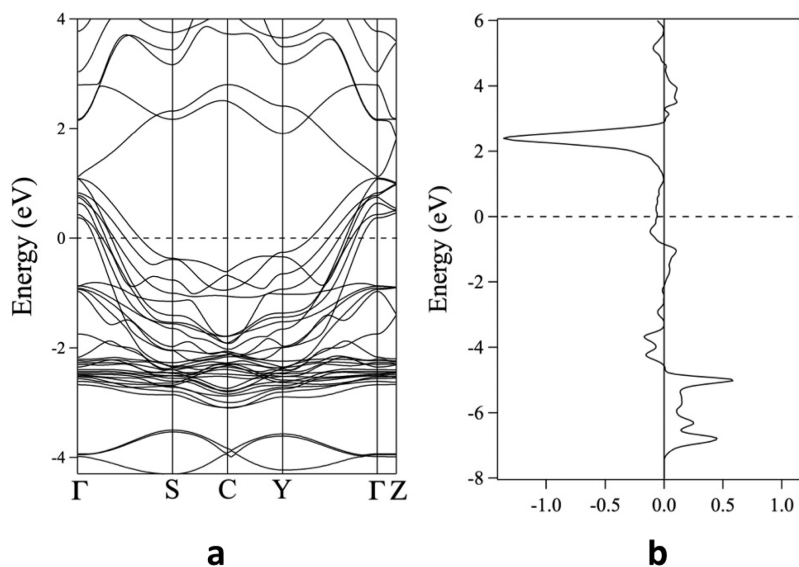


**Figure 4.** (a) Calculated band structure for orthorhombic covellite where  $\Gamma = (0, 0, 0)$ ,  $S = (1/2, 0, 0)$ ,  $C = (1/3, 1/3, 0)$ ,  $Y = (1/2, 1/2, 0)$ , and  $Z = (0, 0, 1/2)$  in units of the reciprocal lattice vectors. (b) COOP curve for the S(2)–S(2) pair.

Because these levels are Cu–S antibonding, these holes provide an additional stabilization to the lattice. Let us note that, although the invocation of Cu 4p<sub>z</sub> mixing to explain the nature of d<sup>10</sup>–d<sup>10</sup> interactions has been questioned,<sup>24</sup> assigning the weak attractive character of these interactions to correlation and relativistic effects, the present bonding situation is clearly different, with Cu 4p<sub>z</sub> mixing involved in the formation of strong three-center interlayer bonds, as revealed by our DFT-based calculations.

Finally, let us note that our analysis immediately highlights the origin of the 55 K structural transition (Figure 1). Distortion toward an orthorhombic structure destroys the 3-fold symmetry axes, and thus the orbitals can no longer be separated into a and e types. Thus, the symmetry lowering allows further orbital mixing, providing an additional, even if small, stabilization of the Cu–S network of covellite. There is no need to invoke additional S··S or Cu··Cu bonding interactions. Because the interactions linking single and double layers are somewhat weaker than those within the layers, it is then understandable that the symmetry lowering can be achieved by a small relative sliding of the two types of layers. The band structure for the orthorhombic phase (Figure 4) shows that the main features found for the hexagonal structure remain practically unchanged after the transition, from which it can be deduced that the same oxidation formalism should be valid for the two known phases of covellite.

In summary, the development of both S–S bonding and S hypervalency not only provides the glue keeping together the two different types of CuS hexagonal layers in covellite but leads to the occurrence of one hole per chemical unit (Cu<sub>3</sub>S<sub>3</sub>) almost equally shared by the different layers present in the structure. Remember that the hypervalency of S(1) implies an S<sup>2-</sup> formal counting for S(1). Because delocalization of the hole affects both the single and double layers and both the Cu and S orbitals, covellite could be described formally either as [(Cu<sup>+</sup>)<sub>2</sub>(S<sub>2</sub><sup>2-</sup>)(Cu<sup>+</sup>)(S<sup>2-</sup>)]-1e or [(Cu<sup>(1+δ)+</sup>)<sub>2</sub>(S<sub>2</sub><sup>2(1-δ)-</sup>)-(Cu<sup>(1+δ)+</sup>)(S<sup>(2-δ)-</sup>)] with δ = 1/6, although neither of these two descriptions does justice to the subtleties of its electronic structure.

## AUTHOR INFORMATION

### Corresponding Authors

\*E-mail: p.alemany@ub.edu.

\*E-mail: canadell@icmab.es.

### Author Contributions

The manuscript was written through contributions of all authors. All authors have given approval to the final version of the manuscript.

### Notes

The authors declare no competing financial interest.

## ACKNOWLEDGMENTS

S.C. gratefully acknowledges the Becas Chile program (CONICYT PAI/INDUSTRIA 72090772) for a doctoral grant. This work was supported by MINECO (Spain) through Grants FIS2012-37549-C05-05, CTQ2012-30751 and CTQ2011-23862-C02-02, and Generalitat de Catalunya (2014SGR301, 2014SGR97, and XRQTC).

## REFERENCES

(1) Isac, L. A.; Duta, A.; Kriza, A.; Enesca, I. A.; Manu, M. *J. Phys.: Conf. Ser.* **2007**, *61*, 477–481.

- (2) Fjellvag, H.; Gronvold, F.; Stolen, S.; Andresen, A. F.; Mueller-Kaefu, R.; Simon, A. *Z. Kristallogr.* **1988**, *184*, 111–121.
- (3) (a) Buckel, W.; Hilsh, R. *Z. Phys.* **1950**, *128*, 324–346. (b) Casaca, A.; Lopes, E. B.; Gonçalves, A. P.; Almeida, M. *J. Phys.: Condens. Matter* **2012**, *24*, 015701.
- (4) Nozaki, H.; Shibata, K.; Ohhashi, N. *J. Solid State Chem.* **1991**, *91*, 306–311.
- (5) (a) Brown, E. C.; York, T. J.; Antholine, W. E.; Ruiz, E.; Alvarez, S.; Tolman, W. B. *J. Am. Chem. Soc.* **2005**, *127*, 13752–13753. (b) Mealli, C.; Ienco, A.; Poduska, A.; Hoffmann, R. *Angew. Chem.* **2008**, *120*, 2906–2910; *Angew. Chem., Int. Ed.* **2008**, *47*, 2864–2868. (c) Alvarez, S.; Hoffmann, R.; Mealli, C. *Chem.—Eur. J.* **2009**, *15*, 8358–8373. (d) Berry, J. F. *Chem.—Eur. J.* **2010**, *16*, 2719–2724. (e) Alvarez, S.; Ruiz, E. *Chem.—Eur. J.* **2010**, *16*, 2726–2728. (f) Ponec, R.; Ramos-Cordoba, E.; Salvador, P. *J. Phys. Chem. A* **2013**, *117*, 1975–1982.
- (6) Liang, W.; Whangbo, M.-H. *Solid State Commun.* **1993**, *85*, 405–408.
- (7) Mazin, I. *Phys. Rev. B* **2012**, *85*, 115133.
- (8) Kumar, P.; Nagarajan, R.; Sarangi, R. *J. Mater. Chem. C* **2013**, *1*, 2448–2454.
- (9) Hohenberg, P.; Kohn, W. *Phys. Rev.* **1964**, *136*, B864–B871. Kohn, W.; Sham, L. J. *Phys. Rev.* **1965**, *140*, A1133–A1138.
- (10) Soler, J. M.; Artacho, E.; Gale, J. D.; García, A.; Junquera, J.; Ordejón, P.; Sánchez-Portal, D. *J. Phys.: Condens. Matter* **2002**, *14*, 2745–2779.
- (11) For more information on the SIESTA code, visit: <http://departments.icmab.es/leem/siesta/>.
- (12) For a review on applications of the SIESTA approach in materials science, see: Sánchez-Portal, D.; Ordejón, P.; Canadell, E. *Struct. Bonding (Berlin)* **2004**, *113*, 103–170.
- (13) Perdew, J. P.; Burke, K.; Ernzerhof, M. *Phys. Rev. Lett.* **1996**, *77*, 3865–3868.
- (14) Troullier, N.; Martins, J. L. *Phys. Rev. B* **1991**, *43*, 1993–2006.
- (15) Kleinman, L.; Bylander, D. M. *Phys. Rev. Lett.* **1982**, *48*, 1425–1428.
- (16) Artacho, E.; Sánchez-Portal, D.; Ordejón, P.; García, A.; Soler, J. M. *Phys. Status Solidi B* **1999**, *215*, 809–817.
- (17) Monkhorst, H. J.; Pack, J. D. *Phys. Rev. B* **1976**, *13*, 5188–5192.
- (18) (a) Morales-García, A.; Lenito Soares, A., Jr.; Dos Santos, E. C.; de Abreu, H. A.; Duarte, H. A. *J. Phys. Chem. A* **2014**, *118*, 5823–5831. (b) Gaspari, R.; Manna, L.; Cavalli, A. *J. Chem. Phys.* **2014**, *141*, 044702.
- (19) Hubbard, J. *Proc. R. Soc. London, Ser. A* **1963**, *276*, 238–257.
- (20) Dudarev, S. L.; Botton, G. A.; Savrasov, S. Y.; Humphreys, C. J.; Sutton, A. P. *Phys. Rev. B* **1998**, *57*, 1505–1509.
- (21) Albright, T. A.; Burdett, J. K.; Whangbo, M.-H. *Orbital Interactions in Chemistry*, 2nd ed.; Wiley: New York, 2013.
- (22) (a) Mehrotra, P. K.; Hoffmann, R. *Inorg. Chem.* **1978**, *17*, 2187–2189. (b) Dedieu, A.; Hoffmann, R. *J. Am. Chem. Soc.* **1978**, *100*, 2074–2079.
- (23) (a) Buljan, A.; Llunell, M.; Ruiz, E.; Alemany, P. *Chem. Mater.* **2001**, *13*, 338–344. (b) Ruiz, E.; Alvarez, S.; Alemany, P.; Evarestov, R. A. *Phys. Rev. B* **1997**, *56*, 7189–7196. (c) Buljan, A.; Alemany, P.; Ruiz, E. *J. Phys. Chem. B* **1999**, *103*, 8060–8066.
- (24) (a) Pyykkö, P.; Zhao, Y.-F. *Angew. Chem., Int. Ed. Engl.* **1991**, *30*, 604–605. (b) Li, J.; Pyykkö, P. *Chem. Phys. Lett.* **1992**, *197*, 586–590. (c) Pyykkö, P.; Mendizabal, F. *Chem.—Eur. J.* **1997**, *3*, 1458–1465. (d) Muñiz, J.; Wang, C.; Pyykkö, P. *Chem.—Eur. J.* **2011**, *17*, 368–377.